

# Solvent Effects on the NMR Parameters of H<sub>2</sub>S and HCN

KURT V. MIKKELSEN,<sup>1</sup> KENNETH RUUD,<sup>2</sup> TRYGVE HELGAKE<sup>2</sup>

<sup>1</sup>Department of Chemistry, University of Copenhagen, DK-2100 Copenhagen Ø, Denmark

<sup>2</sup>Department of Chemistry, University of Oslo, N-0315 Oslo, Norway

Received 1 April 1999; accepted 5 April 1999

**ABSTRACT:** A recently developed method to calculate singlet and triplet gauge-origin-independent magnetic properties of solvated molecules is applied to the study of those parameters that determine an observed nuclear magnetic resonance signal: the magnetizability, the nuclear shieldings, and the indirect spin-spin coupling constants. The solvent is represented by a dielectric medium and the electronic structure of the solvated molecule by Hartree-Fock and multiconfigurational Hartree-Fock wave functions. For the properties that depend on the external magnetic field, we use London atomic orbitals to ensure gauge-origin independence and a rapid basis-set convergence. We find that the dielectric-medium effects on these molecules are substantial, being of the same order as rovibrational and electron correlation effects, and thus cannot be neglected if accurate comparisons with liquid-phase measurements are wanted. However, the present model is incapable of describing the close-range interactions that may occur in solution. It, therefore, represents the electrostatic effects of the bulk solvent, and the model is an initial approach towards a complete *ab initio* model for the study of magnetic properties of solvated molecules. © 1999 John Wiley & Sons, Inc. *J Comput Chem* 20: 1281–1291, 1999

**Keywords:** solvated molecules; NMR parameters; HCN; H<sub>2</sub>S; solvent effects; nuclear magnetic shieldings; spin-spin coupling constants; magnetizabilities; multiconfigurational self-consistent field

## Introduction

During the last decade, there has been an increased interest in the calculation of nu-

Correspondence to: K. Ruud; e-mail: ruud@sdsc.edu  
Contract/grant sponsor: The Norwegian Research Council

clear magnetic resonance (NMR) parameters such as the nuclear shielding constants and the indirect nuclear spin-spin coupling constants. This activity has prompted a number of methodological developments, in particular the adaption of a large number of electron correlation approaches to the calculation of nuclear shieldings and the proposal of different approaches for solving the gauge-origin

problem. For an overview of the developments in *ab initio* calculations of NMR properties of molecules in the gas phase, we refer to a recent review.<sup>1</sup>

However, because most nuclear magnetic resonance experiments take place in the liquid phase, a proper understanding of the observed spectrum can be obtained only if the effects of the surrounding medium are taken into account. We recently presented an approach for calculating the effects of a dielectric medium on molecular properties such as nuclear shieldings and magnetizabilities (using London atomic orbitals to ensure gauge origin independence)<sup>2</sup> and indirect spin–spin coupling constants.<sup>3</sup> In this approach, the molecule is placed in a spherical cavity embedded in the dielectric medium and the polarization energy is evaluated through a multipole expansion. This approach may be contrasted with that of Cremer and coworkers, who combined the Individual Gauges for Localized Orbitals (IGLO) approach with the Polarizable Continuum Model (PCM) for modeling nuclear shieldings of solvated molecules,<sup>4</sup> and also with the London/PCM and Continuous Set of Gauge Transformation (CSGT)/PCM models of Cammi.<sup>5</sup>

The quantum-chemical modeling of the NMR parameters of solvated molecules is still a rather new field, and most investigations have, therefore, been restricted to single-configuration self-consistent field (SCF) wave functions. The only exceptions are the investigations of fluoromethanes<sup>6</sup> and hydrogen selenide,<sup>3</sup> both of which used multiconfigurational SCF wave functions. We also mention the combined molecular dynamics/density-functional theory study of liquid water by Malkin et al.,<sup>7</sup> the combined molecular dynamics/*ab initio* approach by Nyman, Åstrand, and Mikkelsen<sup>8</sup> of liquid water, and the study of solvent effects on the nuclear shieldings and spin–spin couplings of the acetylene molecule by Pecul and Sadlej.<sup>9</sup>

In this article, we investigate the solvent effects on the parameters that determine an observable NMR spectrum (the magnetizability, the nuclear shielding constants, and the indirect spin–spin coupling constants) of two polar molecules: hydrogen sulfide and hydrogen cyanide. We examine the changes in the magnetic properties caused by electron correlation, truncation of the multipole expansion, changes in dielectric constant of the medium, and by solvent geometry relaxation.

In the Theory section, we briefly describe our approach for modeling the dielectric medium effects. In the Computational Data section we give

some computational details, before discussing our results for the magnetizability, nuclear shieldings, and indirect spin–spin coupling constants of hydrogen sulfide and hydrogen cyanide in the Results and Discussion section. The Summary contains some concluding remarks.

## Theory

The field of calculating magnetic properties of gas-phase molecules using London orbitals have in recent years become very popular.<sup>10–13</sup> We have previously described an approach for calculating gauge-origin-independent nuclear shieldings and magnetizabilities of solvated molecules by use of London atomic orbitals.<sup>2,14</sup> In this model, the solute (with optional solvation shells) is placed in a spherical cavity embedded in a homogeneous, linear, and polarizable dielectric medium. The method combines our previous work on developing methods for calculating gauge-origin independent molecular magnetic properties and for determining the solvent effects on molecular properties.<sup>15,13,16–22</sup> The model was recently extended to also treat the effects of triplet-perturbing operators on a solvated molecule, in order to calculate the dielectric-medium effects on indirect nuclear spin–spin coupling constants.<sup>3</sup>

Here, we shall consider the magnetizability  $\xi$ , the nuclear magnetic shielding constants  $\sigma_K$ , and the indirect spin–spin coupling constants  $J_{KL}$  of the solute. These properties may be expressed as derivatives of the molecular energy of the solute:

$$\xi = - \left. \frac{\partial^2 E(\mathbf{B}, \mathbf{m})}{\partial^2 \mathbf{B}} \right|_{\mathbf{B}=\mathbf{m}=0} \quad (1)$$

$$\sigma_K = 1 + \left. \frac{\partial^2 E(\mathbf{B}, \mathbf{m})}{\partial \mathbf{B} \partial \mathbf{m}_K} \right|_{\mathbf{B}=\mathbf{m}=0} \quad (2)$$

and

$$J_{KL} = \left. \frac{\partial^2 E(\mathbf{B}, \mathbf{m})}{\partial \mathbf{m}_K \partial \mathbf{m}_L} \right|_{\mathbf{B}=\mathbf{m}=0} \quad (3)$$

where  $\mathbf{m}_K$  is the nuclear magnetic moment of nucleus  $K$ , and  $\mathbf{B}$  the external magnetic field induction. We have collected all the magnetic moments in  $\mathbf{m} = \{\mathbf{m}_K\}$ .

We represent the outer solvent as a homogeneous, isotropic, and linear dielectric medium. The solute is enclosed by a spherical cavity embedded in this medium. Due to the interaction between the

charge distribution of the solvated molecule and the induced charges in the dielectric medium, we obtain two contributions to the solute's energy functional<sup>18,20–22</sup>

$$E(\mathbf{B}, \mathbf{m}) = E_{\text{vac}}(\mathbf{B}, \mathbf{m}) + E_{\text{sol}}(\mathbf{B}), \quad (4)$$

where  $E_{\text{vac}}(\mathbf{B}, \mathbf{m})$  is the expectation value of the vacuum Hamiltonian and  $E_{\text{sol}}(\mathbf{B})$  is the energy arising from interactions with the dielectric medium. The vacuum part of the energy functional can be written

$$E_{\text{vac}}(\mathbf{B}, \mathbf{m}) = \langle O(\mathbf{B}) | H(\mathbf{m}, \mathbf{B}) | O(\mathbf{B}) \rangle, \quad (5)$$

where we have indicated all explicit dependencies on nuclear magnetic moments and external magnetic fields. The electronic state of the solvated molecule is represented by an MCSCF wave function  $|\text{MC}\rangle$ , parameterized as

$$|\text{MC}\rangle = \exp[-i\kappa] \sum_i C_i |\Theta_i\rangle. \quad (6)$$

The configuration state functions (CSFs)  $|\Theta_i\rangle$  are fixed linear combinations of Slater determinants. Orbital transformations are performed by the unitary operator  $\exp[-i\kappa]$ .

The Hamiltonian of interest for the calculation of NMR parameters may be written as (atomic units used throughout)

$$H(\mathbf{B}, \mathbf{m}) = \frac{1}{2} \sum_i \pi_i^2 - \sum_{iK} \frac{Z_K}{r_{iK}} + \frac{1}{2} \sum_{i \neq j} \frac{1}{r_{ij}} + \frac{1}{2} \sum_{K \neq L} \frac{Z_K Z_L}{R_{KL}} + H^{\text{FC}} + H^{\text{SD}}, \quad (7)$$

where the summations over  $i$  and  $j$  run over all electrons and the summations over  $K$  and  $L$  run over all nuclei. We have also introduced the kinetic momentum

$$\pi_i = -i\nabla_i + \mathbf{A}(\mathbf{r}_i), \quad (8)$$

with the magnetic vector potential representing the external magnetic field and the nuclei given as

$$\mathbf{A}(\mathbf{r}_i) = \frac{1}{2} \mathbf{B} \times \mathbf{r}_{iO} + \alpha^2 \sum_K \frac{\mathbf{m}_K \times \mathbf{r}_{iK}}{r_{iK}^3}, \quad (9)$$

where  $\alpha$  is the fine-structure constant. We have here assumed a static and homogeneous external field and applied the Coulomb gauge. We note that the vector potential depends on the gauge origin  $O$ .

To identify the operators that contribute to the magnetizability, nuclear shielding and spin-spin coupling constants, we expand the square of the kinetic momentum in eq. (7) using eqs. (8) and (9)

$$\begin{aligned} \frac{1}{2} \pi_i^2 = & -\frac{1}{2} \nabla_i^2 + \frac{1}{2} \mathbf{B}^T \mathbf{l}_{iO} + \alpha^2 \sum_K \frac{\mathbf{l}_{iK}^T \mathbf{m}_K}{r_{iK}^3} \\ & + \frac{1}{8} \mathbf{B}^T (r_{iO}^2 \mathbf{I} - \mathbf{r}_{iO} \mathbf{r}_{iO}^T) \mathbf{B} \\ & + \alpha^2 \sum_K \mathbf{B}^T \frac{\mathbf{r}_{iK}^T \mathbf{r}_{iO} \mathbf{I} - \mathbf{r}_{iK} \mathbf{r}_{iO}^T}{r_{iK}^3} \mathbf{m}_K \\ & + \frac{\alpha^4}{2} \sum_{K \neq L} \mathbf{m}_K^T \frac{\mathbf{r}_{iK}^T \mathbf{r}_{iL} \mathbf{I} - \mathbf{r}_{iK} \mathbf{r}_{iL}^T}{r_{iK}^3 r_{iL}^3} \mathbf{m}_L, \end{aligned} \quad (10)$$

where  $\mathbf{I}$  is the  $3 \times 3$  unit matrix.

In the Hamiltonian eq. (7), we have also introduced the Fermi-contact and spin-dipole operators

$$H_K^{\text{FC}} = -\frac{8\pi\alpha^2}{3} \sum_i \delta(\mathbf{r}_{iK}) \mathbf{m}_i, \quad (11)$$

$$H^{\text{SD}} = \alpha^2 \sum_i \frac{r_{iK}^2 \mathbf{m}_i - 3(\mathbf{m}_i \cdot \mathbf{r}_{iK}) \mathbf{r}_{iK}}{r_{iK}^5}, \quad (12)$$

where  $\mathbf{m}_i$  is the electron spin-magnetic moment, related to the electron spin as

$$\mathbf{m}_i = -\frac{1}{2} g_e \mathbf{s}_i, \quad (13)$$

where  $g_e$  is the electron  $g$  factor.

The vacuum contributions to the magnetic properties can now be obtained by differentiating the energy expression eq. (5) with the Hamiltonian described above. To remove the dependence of the Hamiltonian on the global gauge origin, we use London atomic orbitals (LAOs)<sup>23</sup>

$$\omega_\mu(\mathbf{R}_N; \mathbf{A}^e) = \exp(-i\mathbf{A}_N^e \cdot \mathbf{r}) \chi_\mu(\mathbf{R}_N), \quad (14)$$

where  $\chi_\mu(\mathbf{R}_N)$  is an ordinary Gaussian orbital at position  $\mathbf{R}_N$  and  $\exp(-i\mathbf{A}_N^e \cdot \mathbf{r})$  is the London phase factor transforming the global gauge origin into a local gauge origin, chosen to coincide with the position of the nucleus to which the orbital is attached

$$\mathbf{A}_N^e = \frac{1}{2} \mathbf{B} \times \mathbf{R}_{NO}. \quad (15)$$

Integrals over London orbitals are gauge-origin independent, as shown by Helgaker and Jørgensen,<sup>15</sup> although they do depend on a phase origin

(see, for instance, ref. 1 for a more thorough discussion of origin dependencies in calculations using London orbitals).

For the magnetic properties, the solvent contribution to the energy functional can be represented by an equilibrium solvation model<sup>18–22, 24–32</sup>

$$E_{\text{sol}}(\mathbf{B}) = \sum_{lm} g_l (\langle T_{lm} \rangle)^2, \quad (16)$$

where the charge distribution of the solute has been expanded in a multipole series. The charge moments  $\langle T_{lm}(\rho) \rangle$  are expectation values of the nuclear and electronic solvent operators. For a spherical cavity of radius  $R_{\text{cav}}$  embedded in a medium with a static dielectric constant  $\epsilon$ , the  $g_l$  are given by

$$g_l = -\frac{1}{2} R_{\text{cav}}^{-(2l+1)} \frac{(l+1)(\epsilon-1)}{l+(l+1)\epsilon}. \quad (17)$$

The multipole moments  $\langle T_{lm}(\rho) \rangle$  have nuclear and electronic contributions

$$\langle T_{lm} \rangle = T_{lm}^n - \langle T_{lm}^e \rangle. \quad (18)$$

The operators in eq. (18) can be written as

$$T_{lm}^n = \sum_K Z_K R^{lm}(\mathbf{R}_K), \quad (19)$$

$$T_{lm}^e = R^{lm}(r) = \sum_{pq} R_{pq}^{lm} E_{pq}, \quad (20)$$

where the integration over the solid harmonics are given as

$$R_{pq}^{lm} = \langle \phi_p | R^{lm} | \phi_q \rangle. \quad (21)$$

The expectation value of the electronic contributions to the charge moment is

$$\langle T_{lm}^e \rangle = \langle \text{MC} | T_{lm}^e | \text{MC} \rangle = \sum_{pq} D_{pq} R_{pq}^{lm}, \quad (22)$$

where  $|\text{MC}\rangle$  is the reference electronic wave function for our system [see eq. (6)] and  $D_{pq}$  is the one-electron density matrix. The functions  $R^{lm}(\mathbf{R}_K)$  and  $R^{lm}$  are related to the imaginary solid harmonics  $S_l^\mu$ .<sup>18, 22</sup>

The dielectric contribution to the energy functional eq. (4) changes the calculation of the magnetic properties in three ways:

1. The energy functional of the solute eq. (4) is optimized self-consistently in the absence of magnetic-field and nuclear magnetic-

moment perturbations. The solvent contribution changes the molecular orbital and CI coefficients compared with the gas-phase molecule.<sup>22, 20</sup>

2. The solvent Hamiltonian modifies the electronic Hessian that enters the solution of the linear response equations. These additional contributions to the electronic Hessian differ for singlet and triplet response properties.
3. Differentiation of the solvent energy functional with respect to the external magnetic field will introduce reorthonormalization corrections due to the dependence of the atomic basis set on the external magnetic field induction.<sup>2</sup>

We do not go into further details on these additional solvent contributions, referring instead to the articles describing the implementations.<sup>22, 20, 2, 3</sup>

## Computational Details

We have applied the solvent model described in the previous section to investigate the nuclear shieldings, magnetizabilities, and spin–spin coupling constants of  $\text{H}_2\text{S}$  and  $\text{HCN}$ . The results have been obtained using multiconfigurational wave functions. For  $\text{H}_2\text{S}$ , the active space contains six orbitals of  $A_1$  symmetry, four of  $B_1$  and  $B_2$  symmetries, and one orbital of  $A_2$  symmetry, and has previously been used for gas-phase investigations of nuclear shieldings.<sup>16</sup> For  $\text{HCN}$ , we have used the active space of ref. 33, which consists of five orbitals of  $A_1$  symmetry, and two of  $B_1$  and  $B_2$  symmetries. For both molecules, we have kept the core electrons inactive in the calculations. The geometries of the molecules have been optimized in the gas phase and in the solvent using the second-order methods described in refs. 6 and 34. The basis set used is the aug-cc-pVQZ-s0, recently developed for the accurate calculation of nuclear spin–spin coupling constants.<sup>35</sup>

In addition, to investigate the dependence of the nuclear shieldings and magnetizability on the dielectric constants and the truncation of the multipole expansion, we have carried out a number of investigations at the SCF level, using a smaller 6-311++G(2d,2p) basis set.<sup>36</sup> This basis set was chosen for these studies to reduce the computational cost, as this basis is sufficiently accurate for Hartree–Fock studies of magnetizabilities and nuclear shieldings. In all these SCF calculations, we

have optimized the geometries of the solvated molecule for the given dielectric constant and order of the multipole expansion.

As described above, the solvents are in our model characterized by their dielectric constants alone—for our calculations we have chosen the solvents pentane ( $\epsilon = 1.844$ ), benzene ( $\epsilon = 2.28$ ), ethyl acetate ( $\epsilon = 6.02$ ), hexanol ( $\epsilon = 13.3$ ), acetone ( $\epsilon = 20.7$ ), methanol ( $\epsilon = 32.63$ ), and water ( $\epsilon = 78.54$ ). In the correlated calculations, the multipole expansion is always truncated at  $l_{\max} = 10$ . The cavity sizes (radii) used for the two compounds are 4.3 bohr for H<sub>2</sub>S and 4.9 bohr for HCN, which corresponds to the distance from the center of mass to the most distant atom plus the van der Waal radius of that atom.

In addition to investigating the dependence of the isotropic magnetizability and nuclear shieldings of the two molecules on the parameters of the dielectric continuum model, we also separately studied the dependence of the diamagnetic and paramagnetic contributions to the magnetizability and the nuclear shieldings, defined using the natural connection.<sup>37</sup> This connection displays the proper origin dependence and faithfully represent changes in the individual contributions upon solvation, although the convergence of the dia- and paramagnetic contributions themselves might be slower. For the calculation of these dia- and paramagnetic contributions, the center of mass has been used as gauge origin.

For the magnetizability, we investigate not only the isotropic magnetizability but also the anisotropies defined as

$$\Delta\xi_1 = \xi_{aa} - \frac{\xi_{bb} + \xi_{cc}}{2}, \quad (23)$$

$$\Delta\xi_2 = \xi_{bb} - \frac{\xi_{aa} + \xi_{cc}}{2}. \quad (24)$$

Here  $\xi_{aa}$ ,  $\xi_{bb}$ , and  $\xi_{cc}$  are the diagonal elements of the magnetizability tensor,  $\xi_{aa}$  being the smallest and  $\xi_{bb}$  the largest of the three components. For a linear molecule such as HCN, these equations reduce to

$$\Delta\xi = \xi_{\parallel} - \xi_{\perp}. \quad (25)$$

## Results and Discussion

In Table I, we report our gas-phase values for the magnetizabilities, nuclear shieldings, and indirect spin–spin coupling constants for the H<sub>2</sub>S

**TABLE I.**  
Vacuum Values of the Magnetizability, Nuclear Shieldings, and Indirect Spin–Spin Couplings in H<sub>2</sub>S.

Property	SCF	MCSCF	Exp.
$\xi$	−453.6	−457.5	−423 <sup>48</sup>
$\Delta\xi_1$	−53.7	−43.6	
$\Delta\xi_2$	46.5	34.0	
$\sigma_S$	722.3	759.2	$752 \pm 12^{49}$
$\sigma_H$	31.20	30.31	$30.54 \pm 0.01^{50}$
$^1J(\text{HS})$		32.58	
$^2J(\text{HH})$		−13.30	

The magnetizabilities are reported in units of  $10^{-30} \text{ JT}^{-2}$ , and the indirect spin–spin couplings in Hz.

molecule. Similar data for HCN can be found in Table II. All results are reported for the respective optimized geometries. The Hartree–Fock results have been obtained using the 6-311++G(2d,2p) basis, whereas the MCSCF results are calculated using the aug-cc-pVQZ-s0 basis. Because of the well-known triplet instability problem of restricted Hartree–Fock calculations,<sup>1</sup> we do not report Hartree–Fock results for the indirect spin–spin coupling constants. Although the use of different basis sets for the Hartree–Fock and MCSCF calculations means that the changes observed may in part be due to basis set rather than correlation effects, we believe that these effects are rather small.

The effects of electron correlation on the isotropic magnetizability are very small. In agree-

**TABLE II.**  
Vacuum Values of the Magnetizability, Nuclear Shieldings, and Indirect Spin–Spin Couplings in HCN.

Property	SCF	MCSCF	Exp.
$\xi$	−284.2	−281.7	
$\Delta\xi$	−95.4	−91.7	$-126 \pm 13^{51}$
$\sigma_C$	80.77	93.76	$82.1^{52}$
$\sigma_H$	29.64	29.40	$28.32^{53}$
$\sigma_N$	−26.61	16.57	$-20.4^{54}$
$^1J(\text{CN})$		17.98	$26.4^{55}$
$^1J(\text{HC})$		288.9	$267.3^{55}$
$^2J(\text{HN})$		7.27	$12.4^{55}$

The magnetizabilities are reported in units of  $10^{-30} \text{ JT}^{-2}$ , and the indirect spin–spin couplings in Hz.<sup>1</sup>

<sup>1</sup> The experimental spin–spin couplings have been converted from <sup>15</sup>N to <sup>14</sup>N, which is, within the Born–Oppenheimer approximation, related by the ratio of the nuclear magnetogyric ratios only if rovibrational corrections are neglected.

ment with a number of studies,<sup>38–41</sup> electron correlation makes the molecule more diamagnetic. Although the relative changes in the anisotropies are large, the absolute changes remain small. For the shieldings, electron correlation is important for the sulphur shielding, whereas the effect on the hydrogen is very modest, the latter in accordance with the findings of Chesnut.<sup>42</sup> Our MCSCF sulphur shielding is in surprisingly good agreement with the experiment, considering that we would expect the rovibrational corrections to be rather large.<sup>43</sup> Our MCSCF results also compare well with the results of Gauss,<sup>44</sup> who obtained 755.4 ppm at the MP2 level and 735.2 ppm at the CCSD level of theory, considering that our SCF result differ from that of Gauss (713.2 ppm). We would expect a CCSD(T) calculation to fall inbetween the MP2 and CCSD results, being closer to the latter,<sup>1</sup> and thus in good agreement with our MCSCF results assuming the difference in basis set quality to be constant for the different levels of electron correlation.

The difference between theory and experiment observed for the hydrogen shielding is probably due, to a large extent, to rovibrational corrections, although the vibrational corrections found in water are almost twice as large as the deviation we have relative to the experiment for H<sub>2</sub>S.

For HCN, it is interesting to note that this molecule is among the very few molecules for which electron correlation makes the molecule more paramagnetic, another example being acetylene.<sup>41</sup> We also note that electron correlation has a major impact on the nuclear shieldings in this molecule, changing the sign of the nitrogen shielding. However, this is mainly due to the limited size of the active space used in this investigation, reflecting the general overestimation of correlation effects by the CASSCF model, as may be realized in comparison with more sophisticated CCSD(T) calculations,  $-13.6$  ppm.<sup>45</sup> Interestingly, the spin-spin coupling constants are in much better agreement with the experiment than are the shieldings, but we are inclined to believe that this may partly be due to a cancellation of errors in the treatments of the one- and N-electron spaces.

## HARTREE-FOCK CALCULATIONS

### Magnetizability

In Figure 1a, we have plotted the isotropic magnetizability of H<sub>2</sub>S as a function of the dielectric constant of the solvent, along with the diamagnetic

and paramagnetic parts of the magnetizability. As observed for other molecules,<sup>2</sup> an increase in the dielectric constant leads to a diamagnetic shift in the magnetizability. The diamagnetic and paramagnetic contributions both decrease in magnitude with an increase in the dielectric constant. The decrease of the paramagnetic part is, however, about five times larger than the decrease in the diamagnetic part. Thus, it is primarily the paramagnetic magnetizability that determines the solvent behavior of the isotropic magnetizability of the H<sub>2</sub>S molecule.

In Figure 1b, we present the first and second anisotropies of the magnetizability tensor for H<sub>2</sub>S as a function of the dielectric constant of the solvent, relative to the gas-phase values. The first anisotropy first decreases with increasing

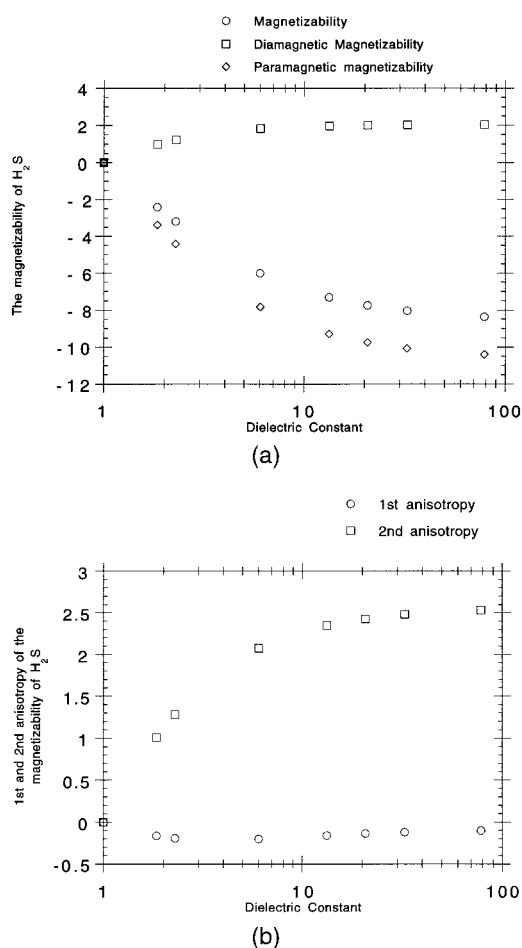


**FIGURE 1.** (a) The isotropic magnetizability of H<sub>2</sub>S vs. the dielectric constant of the solvent. Units are  $10^{-30}$  JT<sup>-2</sup>. (b) The first and second anisotropy of the magnetizability tensor of H<sub>2</sub>S vs. the dielectric constant of the solvent. Units are  $10^{-30}$  JT<sup>-2</sup>.

dielectric constant, but then increases for dielectric constants larger than about 6. However, the changes are small. In contrast, the second anisotropy is more sensitive to the value of the dielectric constant, increasing steadily with increasing dielectric constant.

As for H<sub>2</sub>S—as well as for water and methane<sup>2</sup>—we see from Figure 2 that the isotropic magnetizability of HCN is shifted diamagnetically with increasing dielectric constant. This shift is dominated by the paramagnetic contribution. The solvent shift does not converge until  $l_{\max} \geq 6$ . However, because the extra computational cost for increasing the order of the multipole expansion is negligible, this poses no practical problem, although it demonstrates the inadequacy of the popular Onsager model, where the multipole expansion is truncated at order  $l = 1$ .

### Nuclear Shielding Constants

The solvent-induced shift of the sulphur shielding in H<sub>2</sub>S is rather strong, as can be seen from Figure 3a, with the diamagnetic and paramagnetic contributions oppositely directed (see Fig. 3a). As for water,<sup>2</sup> both contributions are enhanced by the dielectric medium, but the overall shift is dominated by the paramagnetic term. The solvent shift for the hydrogen shielding becomes more negative with increasing dielectric constant (see Fig. 3b). As for H<sub>2</sub>O,<sup>2</sup> the solvent shifts in the paramagnetic and diamagnetic contributions are both diamagnetic (see Fig. 3b), with the diamagnetic term dominating the observed shift, being about four times larger than the paramagnetic term.

○  $l_{\max} = 0$     ×  $l_{\max} = 2$     +  $l_{\max} = 4$     ▽  $l_{\max} = 6$   
 □  $l_{\max} = 1$     ×  $l_{\max} = 3$     △  $l_{\max} = 5$     ■  $l_{\max} = 10$

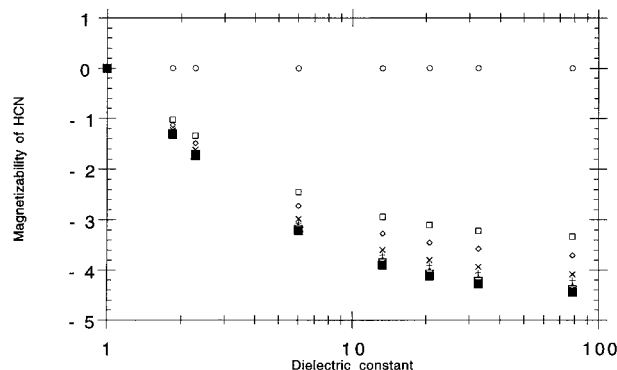


**FIGURE 2.** The isotropic magnetizability of HCN vs. the dielectric constant of the solvent for different truncations of the multipole expansion. Units are  $10^{-30} \text{ JT}^{-2}$ .

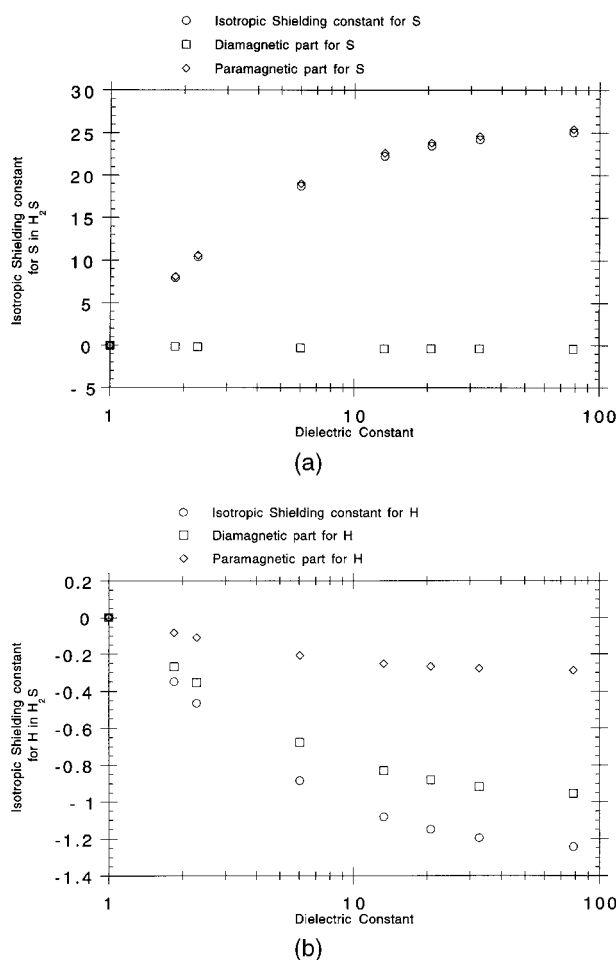


**FIGURE 3.** (a) The isotropic shielding constant along with the dia- and paramagnetic contributions to the isotropic shielding constant for sulphur in H<sub>2</sub>S vs. the dielectric constant of the solvent. Units are ppm. (b) The isotropic shielding constant along with the dia- and paramagnetic contributions to the isotropic shielding constant for hydrogen in H<sub>2</sub>S vs. the dielectric constant of the solvent. Units are ppm.

As seen from Figure 6, the solvent shift of the isotropic hydrogen shielding in HCN decreases with increasing dielectric constant, as was also observed for the hydrogen shifts in H<sub>2</sub>S, H<sub>2</sub>O, and CH<sub>4</sub>.<sup>2</sup> However, the hydrogen shifts in HCN are 10 times larger than for those molecules. The diamagnetic and paramagnetic contributions to the solvent shift of the isotropic hydrogen shielding are both diamagnetic shifts, but it is worth noticing that the shift of the diamagnetic contribution is about 7 times larger than that of the paramagnetic contribution.

Figure 5 shows that the shift of the isotropic carbon shielding in HCN also decreases with in-

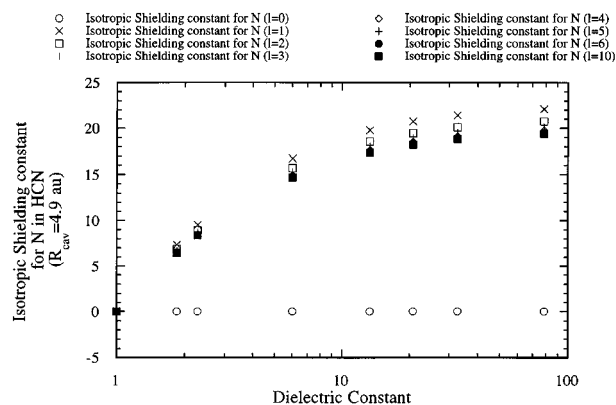


**FIGURE 4.** The isotropic shielding constant for nitrogen in HCN vs. the dielectric constant of the solvent for different truncations of the multipole expansion. Units are ppm.

creasing polarizability of the dielectric medium, converging for multipole expansions with  $l > 4$ . Both the dia- and paramagnetic contributions are shifted diamagnetically, although in this case the solvent shift of the paramagnetic contribution is more than three times larger than the shift of the diamagnetic contribution.

For nitrogen we note in Figure 4 the exceptionally large solvent shift of the isotropic shielding, completely dominated by the shift in the paramagnetic contribution. It is noteworthy that the solvent shifts obtained here are of the same magnitude as the correlation contribution to the nitrogen shielding of HCN,<sup>46</sup> but that these effects oppose each other.

## MCSCF CALCULATIONS

### Hydrogen Sulphide

Our results obtained for the magnetizability, nuclear shieldings, and indirect spin-spin coupling constants using the large basis and the active spaces described in the Computational Details section, is for H<sub>2</sub>S collected in Table III, and for HCN in Table IV.

The effect of solvation is very small on the magnetizability and magnetizability anisotropies of H<sub>2</sub>S. Still, the induced solvent shift in the isotropic magnetizability is larger than the effect of electron correlation. As for the uncorrelated wave functions, the dielectric medium enhances the diamagnetic nature of the molecule. Similarly, anisotropies are unaffected by the presence of the dielectric medium. For all components, the main

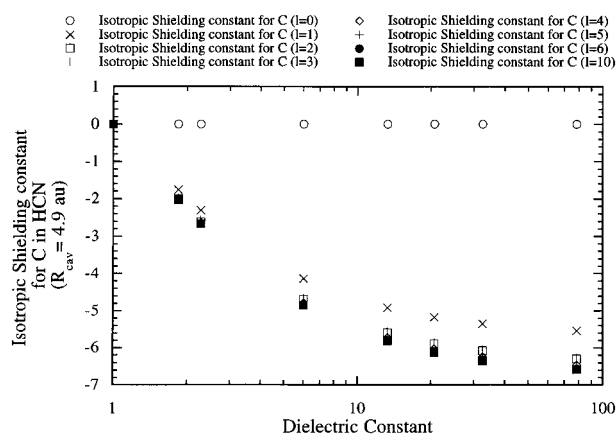


**FIGURE 5.** The isotropic shielding constant for carbon in HCN vs. the dielectric constant of the solvent for different truncations of the multipole expansion. Units are ppm.

effect of the solvent is through polarization of the electronic structure, the difference between the gas phase and solvent geometries being small.

In contrast, both the sulphur and hydrogen shielding constants show a strong dependence on the dielectric medium, with the medium effect amounting to about 3% for both shieldings. The major effect is again due to polarization of the electronic structure of the molecule. Interestingly, the change in geometry enhances the dielectric-medium effect on the sulphur atom for weakly polar solvents ( $\epsilon \leq 6$ ), but reduces it for the more polar solvents. Similarly, the hydrogen shifts are reduced by geometry optimization for the weakly polar media and enhanced in more polar media. For  $\epsilon = 6$ , the geometry relaxation has no effect on

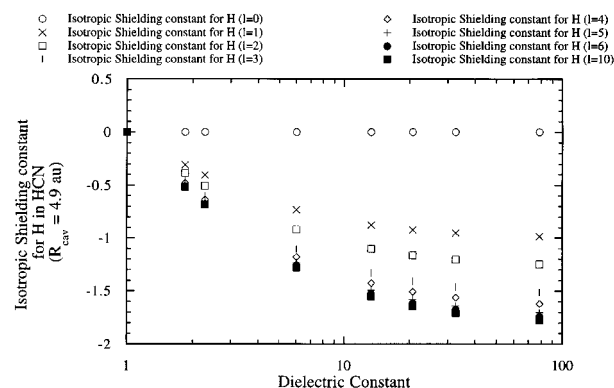


**FIGURE 6.** The isotropic shielding constant for hydrogen in HCN vs. the dielectric constant of the solvent for different truncations of the multipole expansion. Units are ppm.



TABLE III.

Molecular Properties as a Function of the Dielectric Constant, with Gas-Phase (Nonitalic) and Optimized (Italic) Geometries of the H<sub>2</sub>S Molecule.

Dielectric Constant	$\xi$	$\Delta \xi_1$	$\Delta \xi_2$	$\sigma(S)$	$\sigma(H)$	$^1J(HS)$	$^2J(HH)$
1	-457.5	-43.6	34.0	759.2	30.31	32.58	-13.30
1.844	-459.4	-44.0	34.8	768.3	30.02	33.95	-13.58
	-459.4	-44.3	33.8	771.1	30.13	34.11	-14.02
2.28	-460.0	-44.1	35.0	771.1	29.93	34.40	-13.67
	-460.0	-44.4	34.2	773.3	30.01	34.50	-14.04
6.02	-462.1	-44.6	35.8	780.5	29.60	36.01	-13.99
	-462.2	-44.6	35.5	780.5	29.59	35.91	-14.11
13.3	-463.1	-44.7	36.1	784.6	29.40	36.75	-14.14
	-463.3	-44.7	36.0	783.6	29.39	36.56	-14.14
20.7	-463.5	-44.8	36.1	785.9	29.39	36.99	-14.19
	-463.6	-44.7	36.2	784.6	29.33	36.77	-14.15
32.63	-463.7	-44.8	36.2	786.8	29.36	37.16	-14.22
	-463.9	-44.7	36.3	785.3	29.28	36.92	-14.16
78.54	-463.9	-44.8	36.3	787.7	29.32	37.34	-14.25
	-464.2	-44.7	36.4	786.0	29.23	37.08	-14.16

the shieldings. For weakly polar solvents, geometry optimization leads to a reduction of the bond angle and bond lengths, whereas there is an increase in the angle and bond length in polar solvents. Similar observations have been made also for water,<sup>2</sup> and demonstrate the importance of including higher order terms in the multipole expansion. It is worth noting that whereas the dielectric-medium effects are as large as the electron correlation effects on the sulphur shielding, for the hydrogen shieldings, solvation effects are more important.

The same changes in the effect of geometry relaxation can also be seen for the indirect spin-spin coupling constants. For H<sub>2</sub>S, the geometry relaxation enhances the solvent effect for both coupling constants for  $\epsilon \leq 6$  and then slightly decreases it. More interesting is the observation that, for weakly polar solvents, the geometry relaxation dominates the overall solvent shift for the  $^2J(HH)$  coupling. This has also been observed for the hydrogen selenide molecule.<sup>3</sup> The dielectric-medium effects are substantial, being more than 10% for the  $^1J(HS)$  coupling, and 8% for the  $^2J(HH)$  cou-

TABLE IV.

Molecular Properties as a Function of the Dielectric Constant, with Gas-Phase and Optimized Geometries of the HCN Molecule.

Dielectric Constant	$\xi$	$\Delta \xi$	$\sigma(C)$	$\sigma(H)$	$\sigma(N)$	$^1J(HC)$	$^2J(NC)$	$^3J(NH)$
1	-281.7	-91.65	93.76	29.40	116.57	282.6	16.35	5.82
1.844	-282.7	-90.63	91.93	29.06	21.52	285.4	16.79	6.23
	-282.9	-90.61	91.89	28.94	21.48	286.6	16.68	6.17
2.28	-283.0	-90.32	91.37	28.96	23.03	286.2	16.91	6.36
	-283.3	-90.31	91.32	28.79	22.96	287.8	16.76	6.28
6.02	-284.1	-89.33	89.52	28.60	28.01	288.6	17.27	6.78
	-284.6	-89.36	89.35	28.25	27.81	291.9	16.97	6.64
13.3	284.6	-88.9	88.73	28.44	30.13	289.5	17.41	6.96
	285.2	88.98	88.48	28.00	29.86	293.6	17.04	6.79
20.7	284.8	-88.8	88.47	28.38	30.82	289.8	17.46	7.02
	285.4	-88.86	88.20	27.91	30.52	294.2	17.06	6.83
32.63	284.9	-88.7	88.30	28.35	31.28	290.0	17.47	7.05
	285.6	-88.77	88.00	27.85	30.98	294.5	17.07	6.87
78.54	-285.0	-88.61	88.12	28.31	31.77	290.2	17.50	7.09
	-285.7	-88.69	87.79	27.79	31.43	294.9	17.08	6.90

pling. Clearly, for an accurate comparison with experimental determinations in solution, the dielectric-medium effects on the spin-spin couplings cannot be neglected.

### Hydrogen Cyanide

For HCN, the isotropic magnetizability increases (diamagnetically) with increasing dielectric constant. On the other hand, the anisotropy of the magnetizability decreases with the increasing polarity of the solvent. The shieldings of the carbon and hydrogen atoms decrease as the dielectric constant is increased, whereas the shielding of the nitrogen atom increases with increasing dielectric constant. As the dielectric constant increases, the charge distribution of HCN becomes more polar as the dielectric constant increases, and the electronic charge distribution is, therefore, shifted more towards the nitrogen atom and away from the hydrogen and carbon atoms. This leads to a larger shielding at the nitrogen atom and smaller shieldings at the hydrogen and carbon atoms. All the spin-spin coupling constants for HCN increase with increasing dielectric constant. Thinking in terms of a sum-over-states expression for the indirect spin-spin coupling constants, we may explain this behavior as arising from a decrease in the excitation energies of HCN as it is solvated by increasingly more polar dielectric media.

---

### Summary

Buckingham partitioned the solvent contribution  $\sigma_{\text{solvent}}$  to nuclear shielding constants into four contributions<sup>47</sup>

$$\sigma_{\text{solvent}} = \sigma_b + \sigma_a + \sigma_w + \sigma_E. \quad (26)$$

Similar partitioning can be made for the magnetizability and indirect spin-spin coupling tensors. The first term  $\sigma_b$  arises from the magnetic susceptibility of the solvent, and the second term  $\sigma_a$  from the anisotropy of the magnetizability of the solvent molecules in the solvation shells surrounding the solute. The third term  $\sigma_w$  relates to the van der Waal interactions between the solvent molecules and the solute, whereas the last term  $\sigma_E$  accounts for the electrostatic interactions between the solute and the solvent. In this investigation, we have focussed on the latter term  $\sigma_E$  to understand how the dielectric medium induces changes in the magnetic properties of the solvated molecules. In

a recent study on the magnetic properties of fluoromethanes,<sup>6</sup> we have shown that it is necessary to include all four terms to reproduce the experimentally observed shifts.

As noted in ref. 2, we find that the magnetizability for the compounds investigated here becomes more diamagnetic with increasing dielectric constant of the medium (diamagnetic shift), the induced shift being governed primarily by the changes in the paramagnetic contribution to the magnetizability. The solvent-induced shift in the magnetizability strongly depends on the truncation of the multipole expansion of the solute, and we have shown that a restriction of the multipole expansion to the dipole term—the Onsager approximation—gives an insufficient description of the dielectric-medium effects on the magnetizability.

As in our previous studies of solvent effects on the nuclear shieldings,<sup>2,6</sup> we observe that the shielding constant of the most electronegative atom in a compound increases (diamagnetic shift) with increasing dielectric constant, whereas the constants of the other atoms decrease (paramagnetic shift). Except for the hydrogen atom, the solvent effect arises from changes in the paramagnetic contribution to the nuclear shielding constant. The carbon shielding in HCN and the hydrogen shieldings in all investigated molecules decrease with increasing dielectric constant (see also ref. 2). This behavior is related to a decrease in both the paramagnetic and the diamagnetic contributions. For hydrogen, the diamagnetic contribution dominates the solvent shift.

As previously observed,<sup>2,3,6</sup> it is important to use optimized molecular geometries of the solute surrounded by the different solvents. We have observed that the effects due to changes in the geometry may both enhance as well as oppose the effects observed from changes in the dielectric medium alone for a fixed vacuum geometry. In certain cases, in particular for spin-spin coupling constants, the geometry relaxation may dominate the total dielectric medium effect on the magnetic properties.

---

### Acknowledgment

This work has received support from the Norwegian Research Council (Program for Supercomputing) through a grant of computing time. K.V.M. thanks Statens Naturvidenskabelige Forskningsråd for support.

## References

1. Helgaker, T.; Jaszuński, M.; Ruud, K. *Chem Rev* 1999, 99, 293.
2. Mikkelsen, K. V.; Jørgensen, P.; Ruud, K.; Helgaker, T. *J Chem Phys* 1997, 106, 1170.
3. Åstrand, P.-O.; Mikkelsen, K. V.; Jørgensen, P.; Ruud, K.; Helgaker, T. *J Chem Phys* 1998, 108, 2528.
4. Cremer, D.; Olsson, L.; Reichel, F.; Kraka, E. *Isr J Chem* 1993, 33, 369.
5. Cammi, R. *J Chem Phys* 1998, 109, 3185.
6. Åstrand, P.-O.; Mikkelsen, K. V.; Ruud, K.; Helgaker, T. *J Phys Chem* 1996, 100, 19771.
7. Malkin, V. G.; Malkina, O. L.; Steinebrunner, G.; Huber, H. *Chem Eur J* 1996, 2, 452.
8. Nymand, T. M.; Åstrand, P.-O.; Mikkelsen, K. V. *J Phys Chem B* 1997, 101, 4105.
9. Pecul, M.; Sadlej, J. *Chem Phys* 1998, 234, 111.
10. Wolinski, K.; Hinton, J. F.; Pulay, P. *J Am Chem Soc* 1990, 112, 8251.
11. Gauss, J. *Chem Phys Lett* 1992, 191, 614.
12. Schreckenbach, G.; Ziegler, T. *J Phys Chem* 1995, 99, 606.
13. Ruud, K.; Helgaker, T.; Bak, K. L.; Jørgensen, P.; Jensen, H. J. Aa. *J Chem Phys* 1993, 99, 3847.
14. Mikkelsen, K. V.; Ruud, K.; Helgaker, T. *Chem Phys Lett* 1996, 253, 443.
15. Helgaker, T.; Jørgensen, P. *J Chem Phys* 1991, 95, 2595.
16. Ruud, K.; Helgaker, T.; Kobayashi, R.; Jørgensen, P.; Bak, K. L.; Jensen, H. J. Aa. *J Chem Phys* 1994, 100, 8178.
17. Ruud, K.; Helgaker, T.; Bak, K. L.; Jørgensen, P.; Olsen, J. *Chem Phys* 1995, 195, 157.
18. Mikkelsen, K. V.; Dalgaard, E.; Swanstrøm, P. *J Phys Chem* 1987, 91, 3081.
19. Mikkelsen, K. V. *Z Phys Chem* 1991, 170, 129.
20. Mikkelsen, K. V.; Jørgensen, P.; Jensen, H. J. Aa. *J Chem Phys* 1994, 100, 6597.
21. Mikkelsen, K. V.; Luo, Y.; Ågren, H.; Jørgensen, P. *J Chem Phys* 1994, 100, 8240.
22. Mikkelsen, K. V.; Ågren, H.; Jensen, H. J. Aa.; Helgaker, T. *J Chem Phys* 1988, 89, 3086.
23. London, F. *J Phys Radium* 1937, 8, 397.
24. Kim, H. J.; Hynes, J. T. *J Chem Phys* 1992, 96, 5088.
25. Gehlen, J. N.; Chandler, D.; Kim, H. J.; Hynes, J. T. *J Phys Chem* 1992, 96, 1748.
26. Kim, H. J.; Hynes, J. T. *J Chem Phys* 1990, 93, 5194.
27. Felderhof, B. U. *J Chem Phys* 1977, 67, 493.
28. Lee, S.; Hynes, J. T. *J Chem Phys* 1988, 88, 6853.
29. Aguilar, M. A.; del Valle, F. J. O.; Tomasi, J. *J Chem Phys* 1993, 98, 7375.
30. Marcus, R. A. *J Phys Chem* 1992, 96, 1753.
31. Marcus, R. A. *J Chem Phys* 1956, 24, 979.
32. Jortner, J. *Mol Phys* 1962, 5, 257.
33. Rizzo, A.; Helgaker, T.; Ruud, K.; Barszczewicz, A.; Jaszuński, M.; Jørgensen, P. *J Chem Phys* 1995, 102, 8953.
34. Helgaker, T. U.; Almlöf, J.; Jensen, H. J. Aa.; Jørgensen, P. *J Chem Phys* 1986, 84, 6266.
35. Helgaker, T.; Jaszuński, M.; Ruud, K.; Górska, A. *Theor Chem Acc* 1998, 99, 175.
36. Frisch, M. J.; Pople, J. A.; Binkley, J. S. *J Chem Phys* 1984, 80, 3265.
37. Olsen, J.; Bak, K. L.; Ruud, K.; Helgaker, T.; Jørgensen, P. *Theor Chim Acta* 1995, 90, 421.
38. Ruud, K.; Skaane, H.; Helgaker, T.; Bak, K. L.; Jørgensen, P. *J Am Chem Soc* 1994, 116, 10135.
39. Cybulski, S. M.; Bishop, D. M. *J Chem Phys* 1994, 100, 2019.
40. Cybulski, S. M.; Bishop, D. M. *J Chem Phys* 1997, 106, 4082.
41. Ruud, K.; Helgaker, T.; Jørgensen, P. *J Chem Phys* 1997, 107, 10599.
42. Chesnut, D. B. *Chem Phys* 1997, 214, 73.
43. Vaara, J.; Lounila, J.; Ruud, K.; Helgaker, T. *J Chem Phys* 1998, 109, 8388.
44. Gauss, J. *Ber Bunsenges Phys Chem* 1995, 99, 1001.
45. Gauss, J.; Stanton, J. F. *J Chem Phys* 1996, 104, 2574.
46. Gauss, J. *Chem Phys Lett* 1994, 229, 198.
47. Buckingham, A. D.; Schaefer, T.; Schneider, W. G. *J Chem Phys* 1960, 32, 1227.
48. Barter, C.; Meisenheimer, R. G.; Stevenson, D. P. *J Phys Chem* 1960, 64, 1312.
49. Wasylshen, R. E.; Connor, C.; Friedrich, J. O. *Can J Chem* 1984, 62, 981.
50. Raynes, W. T.; Buckingham, A. D.; Bernstein, H. J. *J Chem Phys* 1962, 36, 3481.
51. Gustafson, S.; Gordy, W. *J Chem Phys* 1973, 58, 5181.
52. Jameson, A. K.; Jameson, C. J. *Chem Phys Lett* 1987, 134, 461.
53. Schindler, M.; Kutzelnigg, W. *Mol Phys* 1983, 48, 781.
54. Jameson, C. J.; Jameson, A. K.; Oppusunggu, D.; Wille, S.; Burrell, P. M.; Mason, J. *J Chem Phys* 1981, 74, 81.
55. Dombi, G.; Diehl, P.; Lounila, J.; Wasser, R. *Org Magn Reson* 1984, 22, 573.